ANALYSIS OF COHERENT SYMMETRICAL ILLUMINATION FOR ELECTRONIC SPECKLE PATTERN SHEARING INTERFEROMETRY

Juan F. Román[1], Vicente Moreno[2], Jon N. Petzing[3] and John R. Tyrer[3]

1. Corresponding author. Bayer Diagnostics, Sudbury, CO10 2XQ, Suffolk, UK.
2. Faculty of Physics, University of Santiago de Compostela, 15782, Santiago de Compostela, Spain.
3. Wolfson School of Mechanical and Manufacturing Engineering, Loughborough University, Loughborough, Leics., LE11 3TU, UK.

Abstract

In an effort to find a non-contact technique capable of providing measurements of in-plane strain, the authors designed a speckle shearing interferometer using symmetrical coherent illumination. It is presented the analysis of the sensitivity to displacement and strain of this interferometer, together with the analysis of the phase-stepping of the resultant fringe patterns. A new notation is introduced alongside this analysis to define the interference components in speckle shearing interferometers using multiple illumination beams. Experimental results show the fringe patterns and the phase stepping, in support of the theoretical analysis.

1. INTRODUCTION

Speckle based optical metrology techniques allow whole-field, non-contact and real-time measurement of displacement and strain components [1]. Electronic Speckle Pattern Interferometry (ESPI) is used for the measurement of displacement in the three orthogonal axes, allowing the independent extraction of the two In-Plane displacement (IP) and one Out-Of-Plane (OOP) displacement components. Electronic Speckle Pattern Shearing Interferometry (ESPSI) provides a method for measuring the first spatial derivatives of displacement, these being related to mechanical strain [2-4].

Displacement and strain can be divided into their orthogonal components, the out-of-plane component and the two X and Y in-plane components. If care is taken with the detail of the optical configurations [4-6], then the majority of speckle shearing interferometers can discretely measure the OOP spatial derivative components. However, this is not the case for discrete measurement of the in-plane spatial derivative components, where the issues are more complex. In fact to a certain extent, effort has been expended to identify the disrupting influences of in-plane terms and to remove them from the out-of-plane terms [7].

Extraction of the in-plane terms is possible using aperture based designs and Fourier plane analysis [8] but these systems have yet to be demonstrated as real-time instruments. Extraction of the in-plane terms has also been demonstrated using sequential measurement, changing illumination angles between each data set, thus making it possible to identify the in-plane terms [4, 9-11]. Whilst this approach does work, if the object under study exhibits time varying deformation components, then the approach may not produce the correct result. A solution to this issue has been proposed [12], with a shearing interferometer being designed around three wavelength illumination. The authors in this case demonstrate the extraction of six partial derivatives, but the complexity, overheads and spatial image registration of operating three cameras simultaneously should perhaps not be underestimated

It can therefore be identified that current optical configurations are typically unable to directly measure the in-plane displacement derivative components, isolated from the out-of-plane components, without complex interferometer design. However, a simple technique for the measurement of IP displacement derivative components (and hence strain components) would be of great interest in many engineering applications. Results have been produced which directly measure in-plane strain components, but under special circumstances, such as plane stress or plane strain conditions [13]. Further data [14] has suggested that the use of dual or simultaneous illumination wavefronts may allow direct analysis of in-plane components for arbitrary objects, but this work has not previously been developed any further.

The prediction of the result of speckle interferometers using more than one simultaneous illuminating beam requires careful understanding of the manipulation of the optical properties of speckle, as well as analysis of the geometry of object and image. The standard notation used to describe speckle shearing interferometer output [1,2], reduces the expression for the interference of the optical wavefronts at the observation plane, to a cosine expression that contains the addition of phase delays. However, this does not take into account the relative spatial correlations of the speckle patterns scattered from different incident beams or scattered from different areas of the object, separated by the lateral shear. Furthermore, for a dual beam system, the standard notation used for speckle shearing interferometry does not provide indicators for which wavefronts or which illuminating beams interact, after the lateral shift of the images, or after the absolute value subtraction of the image patterns.

This paper considers in-depth the consequences of using dual beam illumination for deformation analysis within a speckle shearing interferometer, extending previous discussions of this work [15]. The approach taken has been to modify the expression describing the speckle interference pattern so that it is separated into several intensity terms, each one labelled according to which illuminating wavefront contributes to it. These labels take into account the polarisation state of each wavefront, in order to indicate which ones cause interference and which others will just add together their intensities. A generalised notation for the treatment of multi-wavefront speckle interferometers is presented in this work, and it is introduced along with the analysis of the novel interferometer. Initial experimental results are presented which support the development of the theoretical analysis.

2. THEORETICAL ANALYSIS OF DUAL ILLUMINATION

The speckle shearing interferometer used for this study was based on the Michelson design [1], using two mutually coherent and symmetrically incident beams to illuminate the object, as shown in **Error! Unknown switch argument.**. The optical axis of the CCD TV camera bisects the angle made by the two laser illumination beams. For the purposes of the development of the analysis for the simultaneous dual illumination interferometer, it is necessary to individually label wavefront components and consider their amplitude and phase contributions. It should also be noted that as would be expected with a Michelson based optical system, the theoretical development has many initial similarities with existing speckle pattern interferometry theory, although modified and expanded to take into account the nature of the simultaneous illumination.

Both illumination wavefronts in Figure 1 are marked as having the same state of polarisation (in this case vertical polarisation, perpendicular to the plane of incidence). Each wavefront has a different label according to the direction of illumination (Left or Right) and the presence or not of lateral shearing (A or B) applied using the Michelson optics. The L or R label corresponds to the illumination wavefront and the second letter indicates the mirror from which the wavefront was reflected. If we denote the amplitudes (including complex phase) by LA, LB, RA, RB, of the contributory wavefronts arriving to a point (x,y) on the image plane, the intensity will be the result of the product described in equation 1:

$$\mathbf{I}(\mathbf{x},\mathbf{y}) = (\mathbf{LA} + \mathbf{LB} + \mathbf{RA} + \mathbf{RB}) \cdot (\mathbf{LA} + \mathbf{LB} + \mathbf{RA} + \mathbf{RB})^{*} \qquad [\textbf{Error! Unknown switch argument.}]$$

with $$\mathbf{LA} = \|\mathbf{LA}\| \cdot \mathbf{e}^{\mathbf{i}\phi_{LA}}$$ [**Error! Unknown switch argument.**]

$$\mathbf{LA}^* = \|\mathbf{LA}\| \cdot \mathbf{e}^{-\mathbf{i}\phi_{LA}}$$ [**Error! Unknown switch argument.**]

and so on.

That product of the amplitudes with their own conjugate, results in the light intensity at point (x,y), and the result will present any possible constructive or destructive interference, depending on the roughness of the surface responsible for the initial random phase ϕ.

In our notation the optical phase terms ϕ with the sub-index A (ϕ_{LA} and ϕ_{RA}) indicate that these phase terms corresponds to light scattered from point $(x,y)_{OBJECT}$ on the object's surface, arriving to the point $(x,y)_{CCD}$ of the image plane, after being reflected by mirror A. Optical phase terms with the sub-index B (ϕ_{LB} and ϕ_{RB}) indicate that these phase terms correspond to light scattered from point $(x+\delta x,y)_{OBJECT}$ on the object's surface, arriving to the same point $(x,y)_{CCD}$, on the image plane by means of the tilt on mirror B.

The result of the product in equation 1 is shown in equation 4:

$$\begin{aligned}\mathbf{I}(\mathbf{x},\mathbf{y}) = \; & \mathbf{LA}\cdot\mathbf{LA}^* + \mathbf{LA}\cdot\mathbf{LB}^* + \mathbf{LA}\cdot\mathbf{RA}^* + \mathbf{LA}\cdot\mathbf{RB}^* + \\ & \mathbf{LB}\cdot\mathbf{LA}^* + \mathbf{LB}\cdot\mathbf{LB}^* + \mathbf{LB}\cdot\mathbf{RA}^* + \mathbf{LB}\cdot\mathbf{RB}^* + \\ & \mathbf{RA}\cdot\mathbf{LA}^* + \mathbf{RA}\cdot\mathbf{LB}^* + \mathbf{RA}\cdot\mathbf{RA}^* + \mathbf{RA}\cdot\mathbf{RB}^* + \\ & \mathbf{RB}\cdot\mathbf{LA}^* + \mathbf{RB}\cdot\mathbf{LB}^* + \mathbf{RB}\cdot\mathbf{RA}^* + \mathbf{RB}\cdot\mathbf{RB}^*\end{aligned}$$ [**Error! Unknown switch argument.**]

In this expression, the terms of the addition LALA*, LBLB*, RARA* and RBRB* represent the intensity of the beams LA, LB, RA, RB as shown by equation 5:

$$\mathbf{LA \cdot LA^* = \|LA\| \cdot e^{i\phi_{LA}} \cdot \|LA\| \cdot e^{-i\phi_{LA}} = \|LA\|^2}$$ [**Error! Unknown switch argument.**]

and similarly for the rest of the terms.

Mirror B has a small tilt to provide the necessary lateral shearing between the images reflected by mirror A and B. Thus, light incident on the same point of the CCD camera does not come from the same point of the object. Hence, LA and RA will represent the light waves from illumination wavefront L and R respectively, reflected by mirror A and incident on point (x,y) of the CCD plane, coming from the correspondent point (x,y) of the object. Analogously, LB and RB will be the light waves reflected by mirror B (laterally tilted) and incident on point (x,y) of the CCD plane, but with the observation that this light comes from point ($x+\delta x$,y) on the object, due to the tilting of mirror B. This notation allows one to manage the sixteen terms resulting from the interference of four coherent beams that takes place at the image plane.

The rest of the terms can be calculated using the same notation for the amplitude and phase as demonstrated in equation 6, and similarly for the rest of the terms.

$$\begin{aligned}\mathbf{RA}\cdot\mathbf{RB}^* + \mathbf{RB}\cdot\mathbf{RA}^* &= \|\mathbf{RA}\|\cdot\|\mathbf{RB}\|\cdot e^{i\phi_{RA}}\cdot e^{-i\phi_{RB}} + \|\mathbf{RA}\|\cdot\|\mathbf{RB}\|\cdot e^{-i\phi_{RA}}\cdot e^{i\phi_{RB}} \\ &= \|\mathbf{RA}\|\cdot\|\mathbf{RB}\|\cdot\left\{e^{i(\phi_{RA}-\phi_{RB})} + e^{i(\phi_{RB}-\phi_{RA})}\right\} \\ &= \|\mathbf{RA}\|\cdot\|\mathbf{RB}\|\cdot 2\cdot \mathrm{Cos}\left(\phi_{RA}-\phi_{RB}\right)\end{aligned}$$

[**Error! Unknown switch argument.**]

The light intensity registered at a point (x, y) on the CCD camera (image plane) will be the result of the addition of all the terms in equation 4. After manipulation of the mathematical terms, the result can be summarised by equation 7:

$$\begin{aligned}\mathbf{I(x,y)}_{CCD} = {} & \|\mathbf{LA}\|^2 + \|\mathbf{LB}\|^2 + \|\mathbf{RA}\|^2 + \|\mathbf{RB}\|^2 + \\ & \|\mathbf{RA}\|\cdot\|\mathbf{RB}\|\cdot 2\cdot \mathrm{Cos}\left(\phi_{RA}-\phi_{RB}\right) + \\ & \|\mathbf{LA}\|\cdot\|\mathbf{LB}\|\cdot 2\cdot \mathrm{Cos}\left(\phi_{LA}-\phi_{LB}\right) + \\ & \|\mathbf{RA}\|\cdot\|\mathbf{LA}\|\cdot 2\cdot \mathrm{Cos}\left(\phi_{RA}-\phi_{LA}\right) + \\ & \|\mathbf{RA}\|\cdot\|\mathbf{LB}\|\cdot 2\cdot \mathrm{Cos}\left(\phi_{RA}-\phi_{LB}\right) + \\ & \|\mathbf{RB}\|\cdot\|\mathbf{LA}\|\cdot 2\cdot \mathrm{Cos}\left(\phi_{RB}-\phi_{LA}\right) + \\ & \|\mathbf{RB}\|\cdot\|\mathbf{LB}\|\cdot 2\cdot \mathrm{Cos}\left(\phi_{RB}-\phi_{LB}\right)\end{aligned}$$

[**Error! Unknown switch argument.**]

This equation represents the intensity of light at the arbitrary point (x,y) on image plane before any alteration or deformation of the object.

If the object undergoes a static deformation, the intensity pattern registered at the image plane will change accordingly. These movements of the object introduce changes in the optical paths of the four wavefronts (LA, LB, RA and RB) that combine to make the image, and the final image plane speckle pattern will vary.

At this stage, it is assumed that the object deformation is smaller than the average speckle grain size, thus preserving issues of speckle correlation. Deformations bigger than the average size of the speckle grains would introduce a loss of correlation, making very difficult to obtain correlation fringe patterns. In the notation presented here, this imposed condition on the amount of deformation means that the amplitude of the wavefronts at point (x,y) will be the same before and after the deformation of the object, as shown in equation 8:

$$\|\mathbf{LA}\|_{\mathbf{after}} = \|\mathbf{LA}\|_{\mathbf{before}}$$ [**Error! Unknown switch argument.**]

Furthermore, due to the different angles of illumination onto the optically rough surface of the object, and the tilt introduced by mirror B, the intensity and phase of light arriving from mirrors A and B will be different. This implies that:

$$\|\mathbf{LA}\| \neq \|\mathbf{LB}\| \neq \|\mathbf{RA}\| \neq \|\mathbf{RB}\|$$ [**Error! Unknown switch argument.**]

$$\phi_{\mathbf{RA}} \neq \phi_{\mathbf{RB}}$$ [**Error! Unknown switch argument.**]

$$(\phi_{\mathbf{LA}} - \phi_{\mathbf{RA}})_{\mathbf{Before}} \neq (\phi_{\mathbf{LA}} - \phi_{\mathbf{RA}})_{\mathbf{After}}$$ [**Error! Unknown switch argument.**]

Whilst the overall amplitude terms do not change with the movement of the object (equation 8), the in-plane and out-of-plane deformations will introduce phase changes which modify the final speckle pattern. This is recognised when calculating the interference involving sixteen different terms associated with the non-deformed and the deformed state of the object. To a certain extent the complexity of this analysis has parallels to work previously completed concerning wedge and aperture based shearing interferometers [8].

If an arbitrary point (x_0,y_0,z_0) on the object's surface performs a displacement with co-ordinates (u,v,w), the displacement associated to the laterally shifted object point (x_0+δx,y_0,z_0) will be (u+δu,v+δv,w+δw), as shown in Figure 2. Each component of the displacement will introduce a change in the optical path, as indicated in Table **Error! Unknown switch argument.**.

[insert figure 2 here]

[insert table 1 here]

Hence the intensity registered at the same point $(x,y)_{CCD}$ on the image plane after the deformation of the object will be as expressed by equation 12:

$$
\begin{aligned}
I(x,y)^{After}_{CCD} = {} & \|LA\|^2 + \|LB\|^2 + \|RA\|^2 + \|RB\|^2 + \\
& \|RA\| \cdot \|RB\| \cdot 2 \cdot Cos\left(\left[\phi_{RA} + \frac{2\pi}{\lambda}\left(-u \cdot Sin\theta - w \cdot (1 + Cos\theta)\right) \right] - \left[\phi_{RB} + \frac{2\pi}{\lambda}\left(-(u + \delta u) \cdot Sin\theta - (w + \delta w) \cdot (1 + Cos\theta)\right) \right] \right) + \\
& \|LA\| \cdot \|LB\| \cdot 2 \cdot Cos\left(\left[\phi_{LA} + \frac{2\pi}{\lambda}\left(u \cdot Sin\theta - w \cdot (1 + Cos\theta)\right) \right] - \left[\phi_{LB} + \frac{2\pi}{\lambda}\left((u + \delta u) \cdot Sin\theta - (w + \delta w) \cdot (1 + Cos\theta)\right) \right] \right) + \\
& \|RA\| \cdot \|LA\| \cdot 2 \cdot Cos\left(\left[\phi_{RA} + \frac{2\pi}{\lambda}\left(-u \cdot Sin\theta - w \cdot (1 + Cos\theta)\right) \right] - \left[\phi_{LA} + \frac{2\pi}{\lambda}\left(u \cdot Sin\theta - w \cdot (1 + Cos\theta)\right) \right] \right) + \\
& \|RA\| \cdot \|LB\| \cdot 2 \cdot Cos\left(\left[\phi_{RA} + \frac{2\pi}{\lambda}\left(-u \cdot Sin\theta - w \cdot (1 + Cos\theta)\right) \right] - \left[\phi_{LB} + \frac{2\pi}{\lambda}\left((u + \delta u) \cdot Sin\theta - (w + \delta w) \cdot (1 + Cos\theta)\right) \right] \right) + \\
& \|RB\| \cdot \|LA\| \cdot 2 \cdot Cos\left(\left[\phi_{RB} + \frac{2\pi}{\lambda}\left(-(u + \delta u) \cdot Sin\theta - (w + \delta w) \cdot (1 + Cos\theta)\right) \right] - \left[\phi_{LA} + \frac{2\pi}{\lambda}\left(u \cdot Sin\theta - w \cdot (1 + Cos\theta)\right) \right] \right) + \\
& \|RB\| \cdot \|LB\| \cdot 2 \cdot Cos\left(\left[\phi_{RB} + \frac{2\pi}{\lambda}\left(-(u + \delta u) \cdot Sin\theta - (w + \delta w) \cdot (1 + Cos\theta)\right) \right] - \left[\phi_{LB} + \frac{2\pi}{\lambda}\left((u + \delta u) \cdot Sin\theta - (w + \delta w) \cdot (1 + Cos\theta)\right) \right] \right)
\end{aligned}
$$

[Error! Unknown switch argument.]

which may be simplified and rewritten as follows:

Error! Bookmark not defined.

[Error! Unknown switch argument.]

In electronic speckle pattern interferometry, the intensities of the images before and after the deformation of the object are typically recorded by means of a solid state camera and then subtracted in absolute terms, pixel by pixel. The resultant image would have dark speckle fringes at the places where $I^{before}(x,y)=I^{after}(x,y)$. For this to happen with the simultaneous illumination, the six optical phase interference terms which appear in equation 13, must not change the result of the cosine functions and would have to be equal to an even integer number π. These interference terms may be rewritten as Δ_1 to Δ_6 , this transformation being described by equations 14 to 19 respectively:

$$\Delta_1 = \frac{2\pi}{\lambda}\cdot\left(\frac{\partial u}{\partial x}\cdot \mathrm{Sin}\theta + \frac{\partial w}{\partial x}\cdot(1+\mathrm{Cos}\theta)\right)\cdot\delta x$$ [**Error! Unknown switch argument.**]

$$\Delta_2 = \frac{2\pi}{\lambda}\cdot\left(-\frac{\partial u}{\partial x}\cdot \mathrm{Sin}\theta + \frac{\partial w}{\partial x}\cdot(1+\mathrm{Cos}\theta)\right)\cdot\delta x$$ [**Error! Unknown switch argument.**]

$$\Delta_3 = -\frac{4\pi}{\lambda}\cdot u\cdot \mathrm{Sin}\theta$$ [**Error! Unknown switch argument.**]

$$\Delta_4 = -\frac{4\pi}{\lambda}\cdot u\cdot \mathrm{Sin}\theta - \frac{2\pi}{\lambda}\left[\frac{\partial u}{\partial x}\mathrm{Sin}\theta - \frac{\partial w}{\partial x}(1+\mathrm{Cos}\theta)\right]\delta x$$ [**Error! Unknown switch argument.**]

$$\Delta_5 = -\frac{4\pi}{\lambda}\cdot u\cdot \mathrm{Sin}\theta - \frac{2\pi}{\lambda}\left[\frac{\partial u}{\partial x}\mathrm{Sin}\theta + \frac{\partial w}{\partial x}(1+\mathrm{Cos}\theta)\right]\delta x$$ [**Error! Unknown switch argument.**]

$$\Delta_6 = -\frac{4\pi}{\lambda}\cdot u\cdot \mathrm{Sin}\theta - \frac{4\pi}{\lambda}\cdot\frac{\partial u}{\partial x}\cdot \mathrm{Sin}\theta\cdot\delta x$$ [**Error! Unknown switch argument.**]

where δx is lateral shear or shift introduced by mirror B, measured at the object plane.

To obtain a dark pixel (hence a dark correlation fringe) within the subtraction correlation image, the above interference terms must be all simultaneously equal to an even integer number of π. This can only be achieved if certain conditions are satisfied simultaneously:

i) $\Delta_3 = 2m\pi$, where m is the fringe order and can be any integer number. This condition leads to equation 20:

$$2 \cdot u \cdot \mathrm{Sin}\theta = m_1 \cdot \lambda$$ [**Error! Unknown switch argument.**]

where m_1 can be any integer number. This is the equation of the zones of the object with equal *u* (x-axis) in-plane displacement, as seen in in-plane ESPI.

ii) $\Delta_6 = 2m\pi$, m any integer number. If condition *i)* is already satisfied, after some calculation condition *ii)* leads to equation 21:

$$2 \cdot \left(\frac{\partial u}{\partial x}\right) \cdot \delta x \cdot \mathrm{Sin}\theta = m_2 \cdot \lambda$$ [**Error! Unknown switch argument.**]

where m_2 can be any integer number. This is the equation that describes the parts of the object with the same in-plane displacement derivative (strain), $\left(\frac{\partial u}{\partial x}\right)$.

iii) $\Delta_{1,}$ $\Delta_{2,}$ Δ_4, and $\Delta_5 = 2m\pi$. These conditions are all equivalent if *i)* and *ii)* have already been satisfied. After some calculation they can be summarised as equation 22:

$$2 \cdot \left(\frac{\partial w}{\partial x}\right) \cdot \delta x \cdot (1 + \mathrm{Cos}\theta) = m_3 \cdot \lambda$$ [**Error! Unknown switch argument.**]

where m_3 can be any integer number. This is the equation of the zones of the object with the same out-of-plane displacement derivative (slope), $\left(\frac{\partial w}{\partial x}\right)$.

After the digital image subtraction, dark correlation fringes will appear at the zones where the three previous conditions are satisfied simultaneously. The resultant pattern corresponds then to the *moiré* overlapping of three speckle correlation fringe patterns, these being:

- ESPI in-plane displacement fringe pattern.
- in-plane displacement derivative (strain) fringe pattern.
- out-of-plane displacement derivative (slope) fringe pattern.

This *moiré* pattern will appear as a complex mosaic of spots, resulting from the crossing of fringe patterns, as illustrated on **Error! Unknown switch argument.**. The fact that a shearing interferometer results in a moiré related result is not new in itself, with authors having previously presented photographic based systems using Fourier analysis [16,17], to firstly examine out-of-plane terms but also in-plane terms. However, the issues here are to explore optical configurations which result directly in real-time in-plane derivative systems, which lead to extraction of optical phase terms and the potential for quantitative evaluation.

[insert figure 3 about here]

3. ANALYSIS OF OPTICAL PHASE EXTRACTION

Optical phase information extraction is an important issue, because it provides the route forward for eventual generation of quantified data from the instrumentation. By introducing a controlled optical phase shift in one of the illuminating beams of the interferometer, it is possible to perform the phase stepping [18] of the resultant speckle pattern and fringe pattern. If a phase shift (ϕ_{piezo}) is introduced in the optical path of for instance, illumination wavefront L (for this purpose both wavefronts are equivalent), the effect of this phase shift on the interferometer can be calculated analytically by adding the optical phase shift term to all the phases of the wavefronts originated by this beam. With respect to equations 12 and 13, ϕ_{LA} and ϕ_{LB} will change to $\phi_{LA}+\phi_{piezo}$ and $\phi_{LB}+\phi_{piezo}$ respectively. The resultant speckle pattern can then be expressed by equation 23:

Error! Bookmark not defined.

[**Error! Unknown switch argument.**]

Following a similar process of analysis as previously discussed, to obtain a dark pixel (and consequently a dark fringe) after the image correlation subtraction process ($I^{before}(x,y)-I^{after+piezo}(x,y)$), all the six interference terms Δ_i must satisfy several conditions simultaneously:

i) $\Delta_3^{Piezo} = 2m\pi$, where $\Delta_3^{Piezo} = -\frac{4\pi}{\lambda} \cdot u \cdot \mathrm{Sin}\theta - \phi_{PIEZO}$,

and m can be any integer number.

This is equivalent to the condition given by equation [**Error! Unknown switch argument.**:

$$2 \cdot u \cdot Sin\theta + \frac{\phi_{piezo}}{2\pi} \cdot \lambda = m_1' \cdot \lambda$$ [**Error! Unknown switch argument.**]

where m_1' can be any integer number, i.e. the fringe order. As in the case without the phase shifting, this is the equation of the zones of the object with equal *u* (x-axis) in-plane displacement, similar to in-plane ESPI with the phase shift introduced by ϕ_{piezo}.

ii) $\Delta_6^{Piezo} = 2m\pi$, where $\Delta_6^{Piezo} = -\frac{4\pi}{\lambda} \cdot u \cdot Sin\theta - \phi_{PIEZO} - \frac{4\pi}{\lambda} \cdot \frac{\partial u}{\partial x} \cdot Sin\theta \cdot \delta x$, and m is any integer number.

If the condition *i)* has already been satisfied, the first two terms in Δ_6^{Piezo} are equal to Δ_3^{Piezo} and condition *ii)* is fulfilled without the effect of the phase stepping. In this case the result is that the in-plane strain component of the moiré pattern does not phase step.

iii) Δ_1^{Piezo}, Δ_2^{Piezo}, Δ_4^{Piezo} and $\Delta_5^{Piezo} = 2m\pi$.

As in the case before introducing the phase stepping, these conditions are all equivalent if *i)* and *ii)* have already been satisfied and after some calculation they all result in the condition given by equation 25:

$$2\cdot\left(\frac{\partial w}{\partial x}\right)\cdot\delta x\cdot\left(1+\mathrm{Cos}\theta\right)=m_3\cdot\lambda$$ [**Error! Unknown switch argument.**]

indicating that the OOP component of the displacement derivative does not phase step either.

Using similar calculations, it can be demonstrated that the introduction of phase stepping on one of the mirrors on the shearing head, causes the OOP displacement derivative to phase step, while the In-Plane displacement and In-Plane displacement derivative will not phase step.

In summary, the introduction of optical phase stepping in one of the illuminating wavefronts causes the In-Plane displacement pattern to phase step, while the other two components of the moiré pattern (OOP displacement derivative and IP displacement derivative) do not phase step. This property can be used to extract the optical phase information and hence quantitative information, through phase stepping and subsequent phase unwrapping processes.

4. EXPERIMENTAL RESULTS

The purpose of the experimentation has been to demonstrate that the simultaneous dual illumination associated with the speckle shearing interferometer, actually produces the predicted moiré patterns predicted by the theory, and secondly that optical phase stepping techniques can be applied to the interferometer.

The test object chosen for the experimental verification was a split cylinder test or Brazilian Disk, under compressive loading. This consists of a flat disk compressed along its equator and has traditionally been used with techniques such as photoelasticity or moiré interferometry [19] to examine loading and deformation characteristics, although more recent work has been demonstrated using holographic interferometry [20]. A 75mm diameter (6mm thick) Brazilian disk was manufactured from an Araldite™ sheet, and was loaded using a compressive test rig linked to a hydraulic DH-Budenburg dead-weight tester. This provided forces up to 5,000N, with a precision of ±1N.

The Michelson based speckle shearing interferometer used a 50mWatt Nd-YAG laser (wavelength λ=532nm), with a coherence length in excess of 10m. A Pulnix TM-9701 CCD camera was used at the image plane linked through to a MuTech Corporation image processing board. Optical phase-stepping was introduced into the interferometer by means of a piezoelectric actuator supplied Piezo-Systems Jena.

Two sets of validating experiments were initially completed producing different types of results. The first approach was to apply large loads to the disk causing predominant motion out-of-plane with limited in-plane motion. The second approach relied on limited loading of the disk, which resulted in a dominant in-plane motion with limited out-of-plane motion.

Figures 4a to 4d provide examples of the initial experimental analysis of the large loading experiments. The simultaneous dual illumination interferometer produces a speckle based subtraction correlation pattern, which is the result of the inter-crossing of the in-plane displacement rotation signature and the OOP displacement derivative component. From the three expected sub-patterns, the pure in-plane displacement derivative component is missing, due to the fact that the Brazilian Disk was identified as rotating within the compressive testing rig. Also, the only component of the moiré pattern that is affected by the phase stepping is the in-plane displacement component, as predicted in the theoretical analysis.

The second experimental approach produced sets of results showing the disk without rotation and evidence of in-plane displacement derivative data. Figures 5a to 5d provide a sequence of images, which include photoelastic analysis of the disk, as well as interferometric analysis of the disk.. The photoelasticity results were obtained by means of a reflection polariscope (030-series by Measurements Group Inc., North Carolina, USA) consisting of two polariser/quarter-wave assemblies mechanically coupled for synchronous rotation. This optical set-up produces an isochromatic pattern that highlights the distribution of pure in-plane strain, and when overlapped with the ESPI in plane match the moiré pattern obtained with the new interferometer Figures **Error! Unknown switch argument.** d).

The results provide qualitative evidence for the theoretical predictions of the speckle shearing interferometer with two mutually coherent symmetrically incident beams.

5. CONCLUSIONS

In this work the authors present a refinement on conventional Michelson-shearing interferometers, where the use of two simultaneously coherent beams contribute to highlight in-plane strain. In order to predict the final fringe pattern it was necessary to introduce a novel notation. This notation makes it possible to predict the interference of multiple illumination beams in Michelson-shearing interferometers. The calculations using this notation show the prediction for the fringe patterns for a novel interferometer in both stationary state and in the presence of phase-stepping introduced in one of the illuminating beams.

The experiments performed in a Brazilian disk sample show the performance of the novel interferometer and confirm the theoretical predictions for the fringe patterns. The results highlight the pure in-plane strain in the sample studied, in one single measurement with the interferometer. This is an advantage as now a single experiment produces a measurement, instead of having to perform alternative measurements with in-plane ESPI and conventional ESPSI, as the combination of results from two interferometers always produces an increase on the error of the measurement.

References

1/ Rastogi, P.K. (ed.), *Digital speckle pattern interferometry and related techniques*, John Wiley & Sons Ltd, Chichester, 2001.

2/ Leendertz, J. A. and Butters J. N., "An image shearing speckle pattern interferometer for measuring bending moments", *Journal of Physics E*, 6, 1107-1110, 1973.

3/ Hung, Y.Y. and Taylor, C.E., "Measurement of slopes of structural deflections by speckle shearing interferometry", *Experimental Mechanics*, 281-285, 1974.

4/ Steinchen, W. and Yang, L., *Digital Shearography: Theory and Application of Digital Speckle Pattern Shearing Interferometry*, SPIE Press, 2003.

5/ Wan Abdullah, W. S., Petzing, J. N. and Tyrer, J. R., "Wave-front divergence: A source of error in quantified speckle shearing data", *Journal of Modern Optics*, 48, 757-772, 2001.

6/ Ibrahim, J. S., Petzing, J. N. and Tyrer, J. R., "Identifying issues of repeatability in speckle shearing interferometers", *Journal of Measurement Science & Technology* (In-Print), 2004.

7/ Wang, K. F., Tieu, A. K. and Li, E. B., “Influence of in-plane displacement and strain components on slope fringe distributions in double-eaperture speckle wedge shearing interferometry”, *Optics & Laser Technology*, 31, 549-554, 1999.

8/ Sirohi, R. S., *Speckle metrology*, Marcel Dekker Inc, New York, 1993.

9/ Rastogi, P. K., “Measurement of in-plane strains using electronic speckle and electronic speckle-shearing pattern interferometry”, *Journal of Modern Optics*, 43(8), 1577-1581, 1996.

10/ Hung, Y. Y. and Wang, J. Q., “Dual-beam phase shift shearography for measurement of in-plane strains”, *Optics and Lasers in Engineering*, 24, 403-413, 1996.

11/ Aebischer, H. A. and Waldner, S., “Strain distributions made visible with image-shearing speckle pattern interferometry”, *Optics and Lasers in Engineering*, 26, 407-420, 1997.

12/ Kästle, R., Hack, E., and Sennhauser, U., “Multiwavelength shearography for quantitative measurements of two-dimensional strain distributions”, *Applied Optics*, 38(1), 96-100, 1999.

13/ Tyer, J. R. and Petzing, J. N., "In-Plane Electronic Speckle Pattern Shearing Interferometry", 1997, *Optics and Lasers in Engineering*, 26, 395-406.

14/ Petzing, J. N. and Tyrer, J. R., "In-plane electronic speckle pattern shearing interferometry: A theoretical analysis supported with experimental results", *Proceedings of Interferometry '94*, SPIE 2342, 27-36, Warsaw, Poland, 1994.

15/ Román, J. F., Petzing, J. N., and Tyrer, J. R., "Development of Novel Speckle Shearing Interferometers for Direct In-Plane Strain Measurement", *Proceedings of FASIG'98*, Brighton, UK, April 1998.

16/ Patorski, K., "Shearing interferometry and the moire method for shear strain determination", *Applied Optics*, 27(16), 3567-3572, 1988.

17/ Rastogi, P. K., "Direct determination of large in-plane strains using high resolution moiré shearography", *Optics and Lasers in Engineering*, 29, 97-102, 1998.

18/ Robinson, D. W., and Reid, G. T., *Interferogram analysis: Digital fringe pattern measurement techniques*, IOP Publishing Ltd., Bristol, 1993.

19/ Dally, J. W. and Riley, W. F., *Experimental stress analysis*, McGraw-Hill International Editions, New York, 1991.

20/ Castro-Montero, A., Jia, A., and Shah, S.P. ,"Evaluation of damage in Brazilian test using holographic interferometry", *American Concrete Institute Materials Journal*, 92(3), 268-275, 1995

Tables of Results

Mirror	**Component of the Displacement**	**Optical Path Change in Beam L**	**Optical Path Change in Beam R**
A	u (X axis)	+ u·Sinθ	- u·Sinθ
A	v (Y axis)	*nil*	*nil*
A	w (Z axis)	- w·(1+Cosθ)	- w·(1+Cosθ)
B	u+δu (X axis)	+ (u+δu)·Sinθ	- (u+δu)·Sinθ
B	v+δv (Y axis)	*nil*	*nil*
B	w+δw (Z axis)	- (w+δw)·(1+Cosθ)	- (w+δw)·(1+Cosθ)

Table **Error! Unknown switch argument.**. Optical path changes in double beam interferometer.

Figure Captions

Figure **Error! Unknown switch argument.** Speckle shearing interferometry with two mutually coherent symmetrically incident beams.

Figure **Error! Unknown switch argument.**. Different position and displacement vectors in ESPSI with two mutually

coherent symmetrically incident beams.

Figure **Error! Unknown switch argument.**. Moiré overlapping of two speckle patterns.

Figures **Error! Unknown switch argument.**(a-d). Same sample subjected to the same force, a) ESPI in plane result, b) OOP strain, c) fringe pattern with the new interferometer, d) results of phase stepping with new interferometer. Note how patterns a) and b) overlap to produce the result with the new interferometer.

Figures **Error! Unknown switch argument.**(a-d). The overlapping of the results of photoelasticity (in plane strain), a) and b) and ESPI In Plane, c) is analogous to the fringe pattern obtained independently with the two beam interferometer, d).

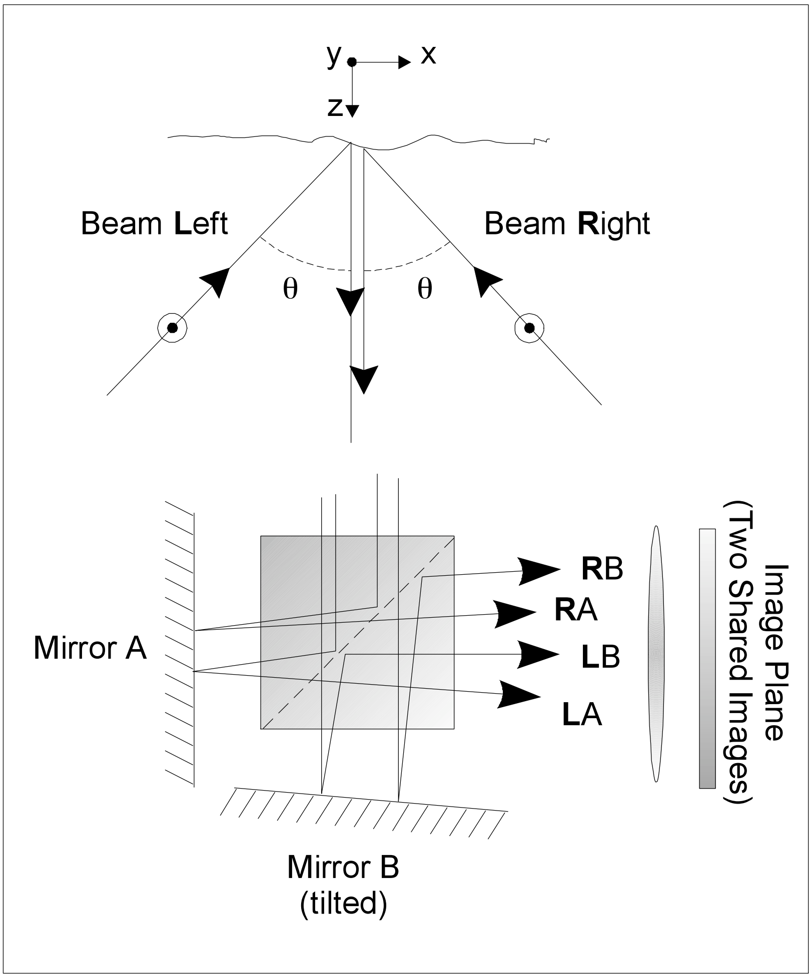
y
x
z
Beam Left
Beam Right
θ
θ
Mirror A
RB
RA
LB
LA
Image Plane
(Two Shared Images)
Mirror B
(tilted)

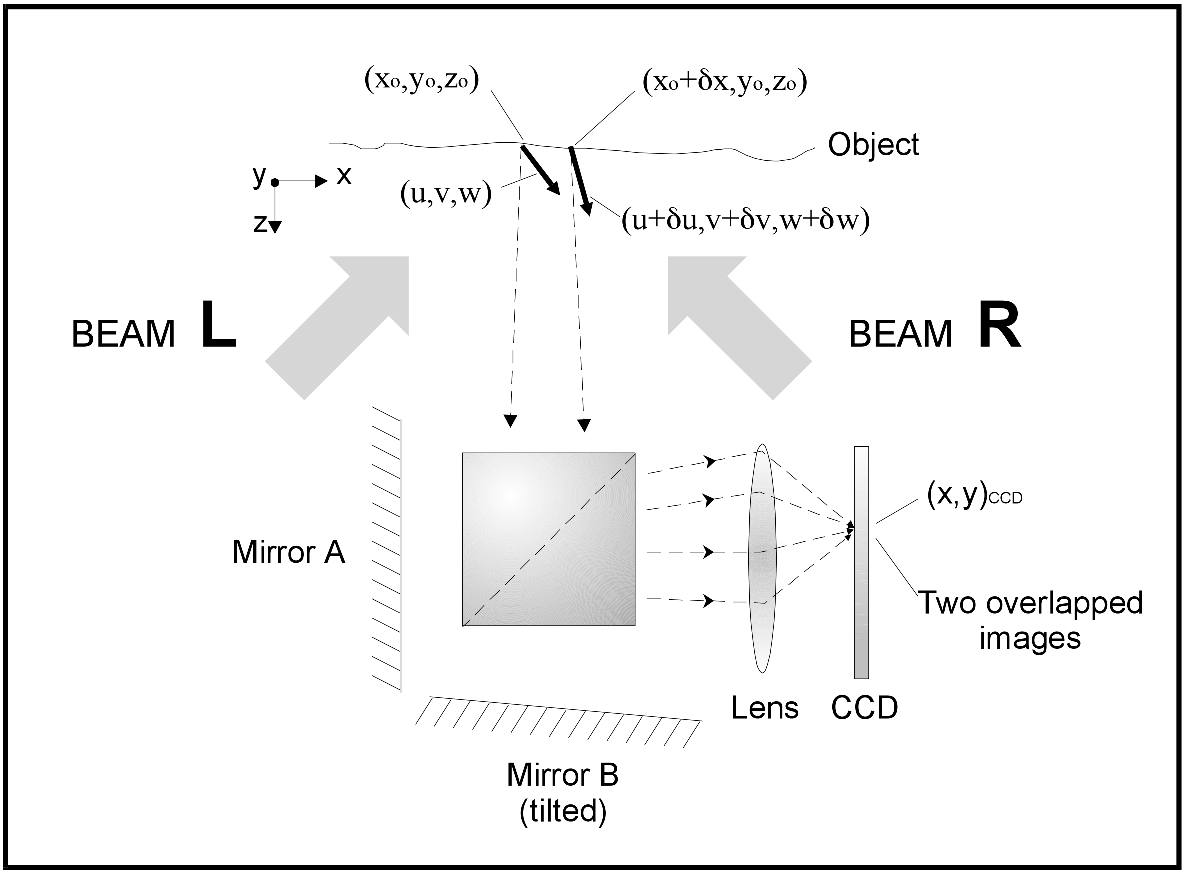
(xo,yo,zo)
(xo+δx,yo,zo)
Object
y
x
z
(u,v,w)
(u+δu,v+δv,w+δw)
BEAM L
BEAM R
Mirror A
(x,y)CCD
Two overlapped images
Lens
CCD
Mirror B (tilted)

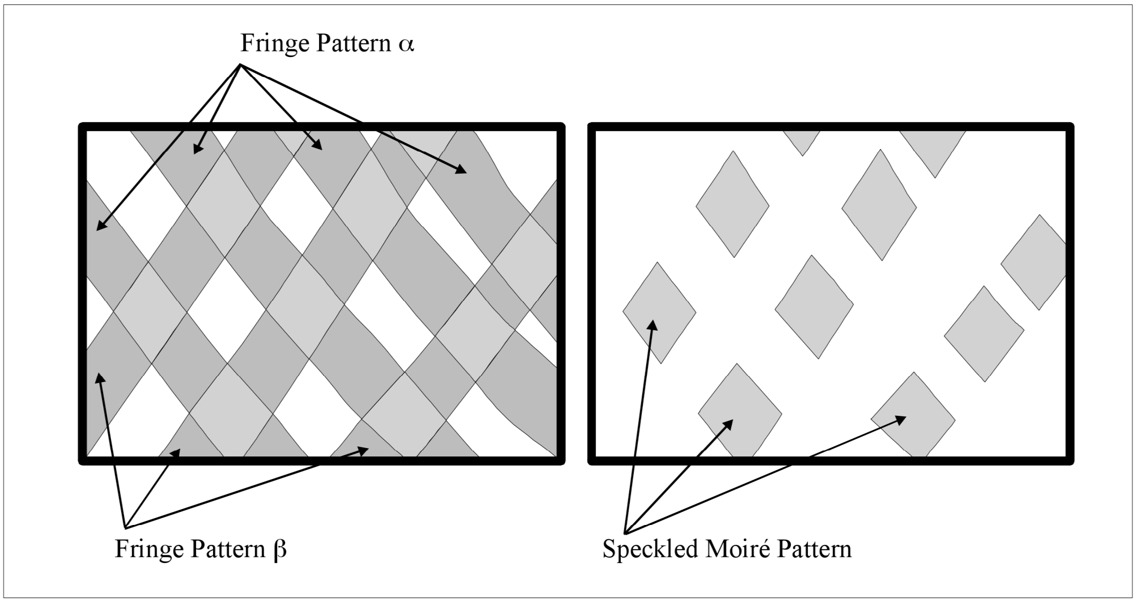
Fringe Pattern α
Fringe Pattern β
Speckled Moiré Pattern

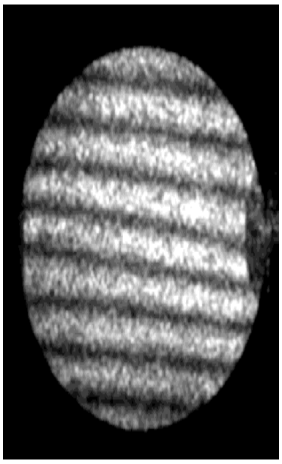

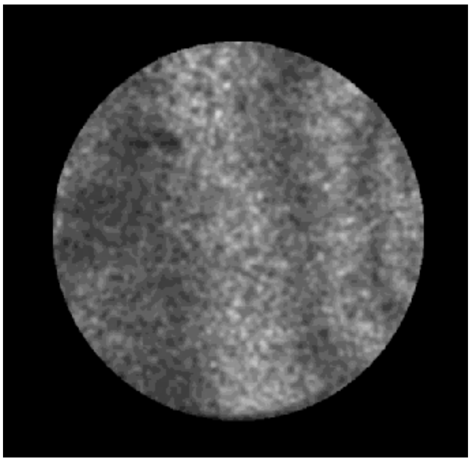

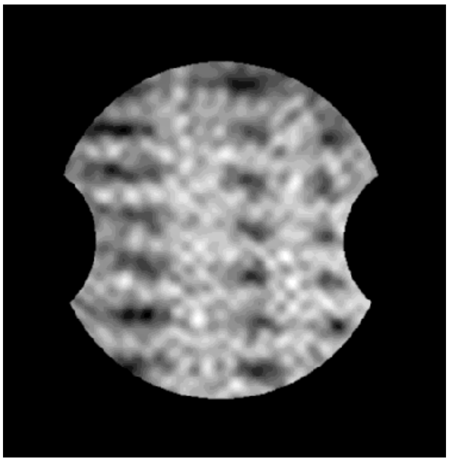

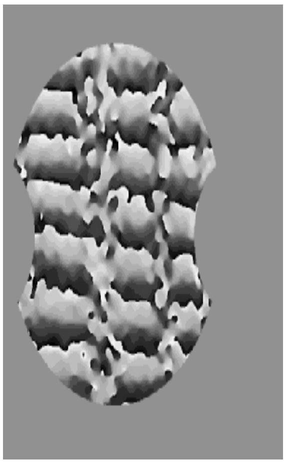

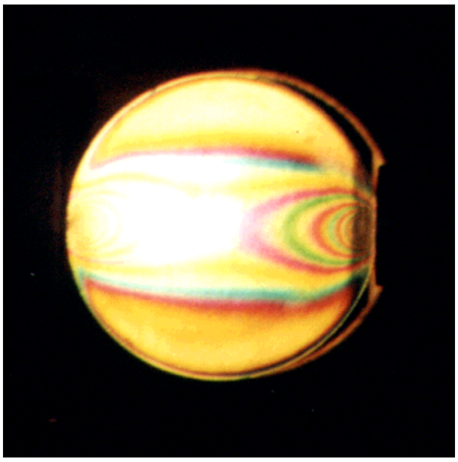

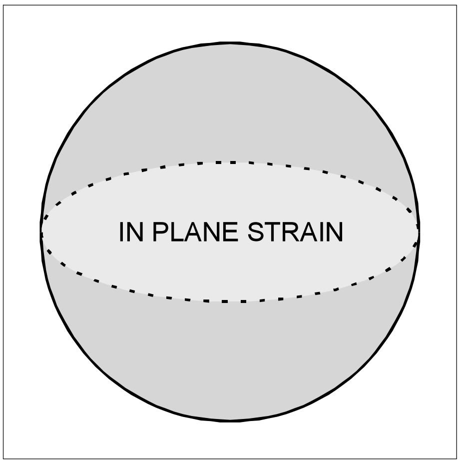
IN PLANE STRAIN

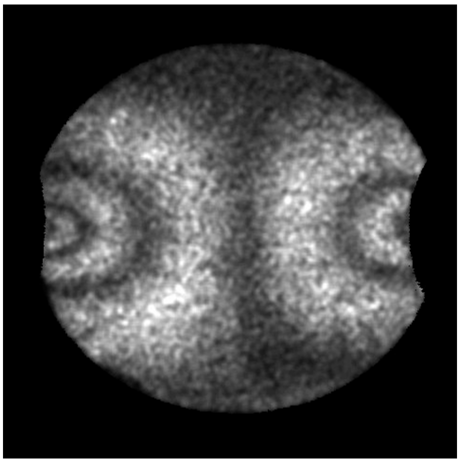

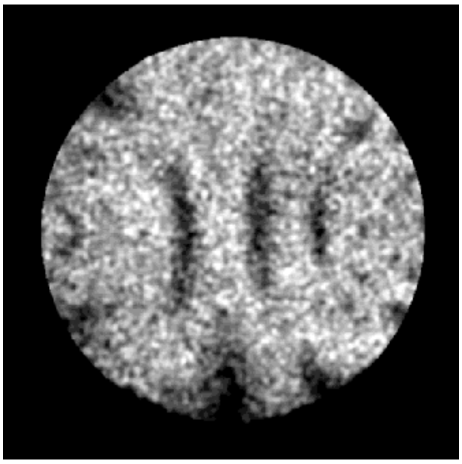

479